OPEN

Light: Science & Applications (2015) 4, e320; doi:10.1038/lsa.2015.93

www.nature.com/lsa

ORIGINAL ARTICLE

Exploring new avenues in high repetition rate table-top coherent extreme ultraviolet sources

Steffen Hädrich[1,2], Manuel Krebs[1], Armin Hoffmann[1], Arno Klenke[1,2], Jan Rothhardt[1,2], Jens Limpert[1,2] and Andreas Tünnermann[1,2,3]

The process of high harmonic generation (HHG) enables the development of table-top sources of coherent extreme ultraviolet (XUV) light. Although these are now matured sources, they still mostly rely on bulk laser technology that limits the attainable repetition rate to the low kilohertz regime. Moreover, many of the emerging applications of such light sources (e.g., photoelectron spectroscopy and microscopy, coherent diffractive imaging, or frequency metrology in the XUV spectral region) require an increase in the repetition rate. Ideally, these sources are operated with a multi-MHz repetition rate and deliver a high photon flux simultaneously. So far, this regime has been solely addressed using passive enhancement cavities together with low energy and high repetition rate lasers. Here, a novel route with significantly reduced complexity (omitting the requirement of an external actively stabilized resonator) is demonstrated that achieves the previously mentioned demanding parameters. A krypton-filled Kagome photonic crystal fiber is used for efficient nonlinear compression of 9 μJ, 250 fs pulses leading to ~7 μJ, 31 fs pulses at 10.7 MHz repetition rate. The compressed pulses are used for HHG in a gas jet. Particular attention is devoted to achieving phase-matched (transiently) generation yielding $>10^{13}$ photons s^{-1} (>50 μW) at 27.7 eV. This new spatially coherent XUV source improved the photon flux by four orders of magnitude for direct multi-MHZ experiments, thus demonstrating the considerable potential of this source.
Light: Science & Applications (2015) **4,** e320; doi:10.1038/lsa.2015.93; published online 28 August 2015

Keywords: coherent extreme ultraviolet sources; high average power; high harmonic generation; nonlinear compression; ultrafast laser

INTRODUCTION

High harmonic generation (HHG) offers an elegant approach to achieve table-top sources of coherent extreme ultraviolet (XUV) or even soft X-ray radiation[1]. Although this process has been known for almost 30 years, it is still a subject of intense research because of the ever-increasing number of possible applications. Moreover, these sources are an alternative to large-scale facilities, such as free electron lasers or synchrotrons, which provide limited user access. All of these sources are used in diverse fields, e.g., in physics, biology, chemistry, material science, and others. This application-oriented approach has defined two major challenges in the field of HHG, which involved either increasing the energy per XUV pulse or the repetition rate[2,3]. The latter challenge is particularly important for photoelectron spectroscopy and microscopy in which space-charge effects need to be avoided[3,4]. Other possible applications are coherent diffractive imaging[5,6], coincidence experiments[7], or frequency metrology, in which multi-10 MHz lasers with a stabilized frequency comb are used[8]. Generally, there is a great demand for compact, cost-effective and reliable sources that can also be used by scientists who are not laser experts, which would severely broaden their applications.

HHG relies on the interaction of a high-intensity (10^{13}–10^{15} W cm^{-2}) ultrashort laser pulse with noble gases. The efficiency of the HHG process critically depends on the possibility of achieving phase-matching, i.e., matching the phase velocity of the driving laser field and the generated XUV field[9]. The phase-mismatch is determined by the dispersion of the neutral atoms and free electrons, the intrinsic phase due to the propagation of the free electron wave-packet as well as a geometrical term, which is caused by the Gouy phase-shift[10,11]. The dispersion terms (neutral atoms, free electrons) have opposite signs and are density dependent. Therefore, phase-matching can be transiently achieved (i.e., for a certain instance of time of the laser pulse) by adjusting the pressure of the generation gas to balance the terms. However, this approach only works when the ionization of the gas medium is maintained below a so-called critical ionization, which is a few percent depending on the gas species and harmonic order[1,9]. This critical ionization level restricts the intensity that can be used for HHG to a maximum value that significantly increases with decreasing pulse duration. Consequently, ultrashort pulses (<10 cycles) will allow the use of a higher intensity, which in turn increases the single atom response while still achieving phase-matching and high efficiencies ($>10^{-6}$)[1]. Therefore, the Ti:Sapphire-based laser systems, due to their ultrashort pulse duration, are still considered the work horse in this field[1].

However, due to the thermo-optical constraints, the repetition rate does not exceed a few kilohertz (a few Watt of average power).

[1]Friedrich-Schiller-Universität Jena, Institute of Applied Physics, Abbe Center of Photonics, Albert-Einstein-Straße 15, 07745 Jena, Germany; [2]Helmholtz-Institute Jena, Fröbelstieg 3, 07743 Jena, Germany and [3]Fraunhofer Institute for Applied Optics and Precision Engineering, Albert-Einstein-Straße 7, 07745 Jena, Germany
Correspondence: Steffen Hädrich, Email: steffen.haedrich@uni-jena.de
Received 28 October 2014; revised 7 April 2015; accepted 8 April 2015; accepted article preview online 13 April 2015

However, novel laser concepts, such as thin-disk[12,13], innoslab[14], and fiber lasers[15], have shown impressive advances in their performance and reached the kilowatt level of average power during pulsed operation. All of these architectures are based on ytterbium-doped laser materials that limit the attainable pulse duration to a few hundred femtoseconds. Nevertheless, early experiments on HHG with fiber lasers have already indicated the great potential of these sources[16,17], which has also been validated by the recently measured photon flux of 4.5×10^{12} photons s^{-1} over several harmonics at 100 kHz repetition rate[18]. However, as noted above, the rather long pulse duration hinders efficient HHG, suggesting the need for post-compression techniques, such as nonlinear compression in noble gas-filled glass capillaries[19]. Nonlinear compression has already shown its capability to be operated with high average powers[20]. Additionally, the use of fiber-chirped pulse amplifiers in combination with nonlinear compression progressively increases the photon flux obtained via HHG. More than 3×10^{13} photons s^{-1} per harmonic (140 μW) at 30 eV[21] and more than 3×10^{9} photons s^{-1} within a 1% bandwidth at 120 eV[22] have been generated recently, which can now be considered the highest photon flux HHG sources in this spectral range. The repetition rate in those experiments was 600 kHz and 100 kHz, respectively, but a further increase to the multi-MHz level is required to address the previously mentioned applications.

To meet this requirement, passive external resonators that enhance the incoming power by a factor of up to 1000 have been proposed. Therefore, a low energetic laser system can be employed at repetition rates ranging from 10 MHz[23] to 154 MHz[8]. However, they require an active stabilization of the resonator to maintain the enhancement. Moreover, the harmonics have to be generated directly in the resonator, which necessitates an out-coupling mechanism for the harmonics, adding additional experimental complexity[8,24]. The occurring ionization of the generation gas puts further constraints on the achievable enhancement and phase-matching conditions that challenges further development[24,25]. A second approach relies on plasmonic field enhancement that potentially allows operation directly with laser oscillators[26]. Here, a specially designed nanostructure leads to field enhancement near the edges of these structures that can provide the required intensity for HHG. However, the usability of the latter is heavily debated in the community, and it remains unclear whether this approach is feasible[27]. A third possibility is to directly use high repetition rate laser systems. This requires tighter focusing to achieve the intensities necessary for HHG, which also severely increases the contribution of the geometrical phase-mismatch term (see above). In combination with the reduced focal spot size and generation volume, it has been suggested that the efficiency will be significantly lower than in loose focusing geometries[28]. Indeed, the lack of phase-matching explains the poor efficiency of previous multi-MHz repetition rate sources that do not deliver more than a few 10^{8} photons s^{-1} in a single harmonic[28,29]. However, investigations of the phase-matching behavior suggest that this can be overcome by properly choosing the experimental conditions, most notably a high-density gas target, to achieve the same pressure-length product as in loose focusing geometries[10,11]. Recent experiments have successfully demonstrated efficient conversion (8×10^{-6}) in a tight focusing geometry[11].

In this article, nonlinear compression of 9 μJ, 250 fs pulses in a krypton-filled Kagome photonic crystal fiber (PCF) is demonstrated. After spectral broadening in the PCF, ~7 μJ, 31 fs pulses are achieved at up to 10.7 MHz repetition rate. This laser system is used to demonstrate transiently phase-matched HHG. More than 10^{13} photons s^{-1} (>50 μW) are achieved in a single harmonic at 27.7 eV, which is an improvement of four orders of magnitude for a directly driven multi-MHz repetition rate HHG[28,29], and it provides a photon flux that is higher than that delivered by standard kHz laser systems[30] and intracavity HHG within that wavelength range[8,24,31]. The use of a low-energy driving laser with a compact nonlinear compression setup not only has the potential to significantly reduce the complexity of high repetition rate HHG systems but will also enable efficient HHG at 10 MHz repetition rate, a regime so far only addressable with enhancement cavities.

MATERIALS AND METHODS

The experimental setup of the nonlinear compression stage followed by a HHG experiment is shown in Figure 1. The front end is a fiber chirped pulse amplification system that optionally allows for the coherent combination of up to four main amplifier channels (CC-FCPA)[32]. This system is chosen because of its short pulse duration of 250 fs, which also enables shorter pulses after the nonlinear compression.

It is important to emphasize that only 8–9 μJ of pulse energy is used at up to 10.7 MHz repetition rate (90 W average power). Therefore, this system, which was used due to its availability, can be easily replaced by compact, turn-key fiber laser systems[33,34] or with state-of-the-art thin-disk oscillators[35,36]. The nonlinear compression stage is necessary to achieve the required ultrashort pulse durations for efficient HHG[1,9]. The pulses from the CC-FCPA are directed through a telescope and a focusing lens and are then coupled into the Kagome fiber (Figure 1). This new type of PCF offers a relatively large core (30–60 μm), low propagation loss and allows studying a variety of nonlinear effects[37]. Interestingly, the Kagome PCF has been recognized as the perfect waveguide for nonlinear compression of μJ-level pulses[38,39], whereas conventional capillaries have extremely high propagation losses due to the required small diameter. Furthermore, they can be operated at high average powers[40]. Here, a commercially available Kagome (PMC-C-Yb-7C, GLOphotonics Limoge, France) with a mode-field diameter of 40 μm and a length of 1 m is used. The Kagome

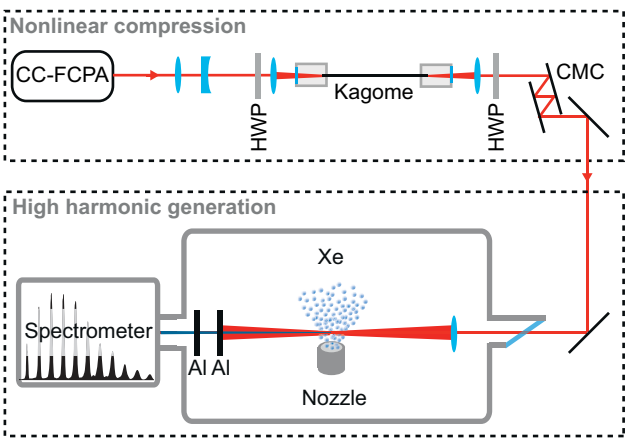

Figure 1 The pulses from a fiber chirped pulse amplifier (CC-FCPA) are coupled into a 1 m long Kagome PCF, which is filled with krypton gas. After spectral broadening, the pulses are compressed by a chirped mirror compressor and then directed to a vacuum chamber for HHG. A lens focuses the pulses to an intensity of 7.4×10^{13} W cm^{-2} (11 μm focal spot radius) in a xenon gas jet ejected from a nozzle, which is mounted on an x-y-z translation stage. Two 200 nm thick aluminum filters separate the generated harmonics and the remaining infrared light. The spatial-spectral analysis of the harmonics is performed with a flat-field grating spectrometer (HWP – half wave plate).

doi:10.1038/lsa.2015.93

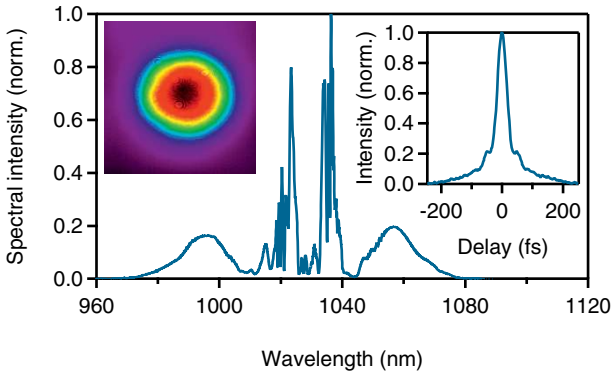

Figure 2 The broadened spectrum at a repetition rate of 10.7 MHz (Left inset: beam profile of the collimated beam. Right inset: autocorrelation of the compressed pulse).

fiber is mounted on a water-cooled V-groove to ensure stable high average power operation. Before coupling into the fiber, a first half-wave plate (HWP) adjusts the polarization so that linear polarization is obtained behind the fiber. Subsequently, another HWP rotates to p-polarization, which is required for the chirped mirror compressor (Figure 1). Typically, approximately 3% of the emitted power is found to be in the incorrect polarization direction when operating the setup as described here. This excellent linear polarization, in addition to ultrashort pulses, is a crucial prerequisite for achieving efficient HHG[41].

The average power transmission through the setup is greater than 80% including coupling, propagation, and the mirror compressor. To achieve spectral broadening, the fiber is statically filled with 7 bar of krypton gas. When coupling the ~9 μJ pulses into the fiber, self-phase modulation in the krypton gas produced a rms-bandwidth of approximately 49 nm after the fiber (Figure 2). Further spectral broadening was not possible with this specific fiber due to the occurrence of other nonlinear effects. However, it has already been demonstrated that proper fiber designs allow for the achievement of 10 fs pulses[39]. Temporal compression is then achieved using four reflections on highly dispersive and broadband (-350 fs^2 per reflection, 980–1080 nm) chirped mirrors. The compressed pulse is characterized by an autocorrelation width of ~43 fs (inset in Figure 2) that corresponds to a pulse duration of ~31 fs (transform-limit: 30 fs). The energy of the compressed pulse is 7.1 μJ (76 W average power at 10.7 MHz). Approximately 70% of the total energy (including pre-/post-pulses of the CC-FCPA) is contained in the main pulse, leading to a peak power of approximately 140 MW. Due to the use of a waveguide for spectral broadening, the spatial quality of the output beam is excellent as indicated by the collimated beam profile after the chirped mirror compressor (inset in Figure 2).

After this nonlinear compression stage, the pulses are steered into a vacuum chamber for HHG (Figure 1). A Brewster-angled entrance window is used to eliminate reflection losses. The beam is focused to a radius ($1/e^2$-intensity) of ~11 μm, leading to an estimated peak intensity of 7.4×10^{13} W cm^{-2}. The noble gas for HHG is injected by a 65 μm nozzle continuously backed with xenon at several bar of pressure. The choice of the gas jet size is explained in more detail in the following section (Results and Discussion). After the HHG, the fundamental laser beam and the XUV light co-propagate until a pair of 200 nm thick aluminum filters reflect the laser light and partly transmit the harmonics, which are then analyzed with a flat-field grating spectrometer to observe the spatial and spectral characteristics.

The average power of the harmonics is obtained by spatially and spectrally integrating over a single harmonic and accounting for the transmission characteristics of the detection system as described in Ref. 21. This includes the diffraction efficiency of the spectrometer grating, the characteristics of the detector (CCD, characterized by the manufacturer) and the measured filter transmission (see Supplementary material).

RESULTS AND DISCUSSION

The optimization of the experimental conditions is performed at 234 kHz repetition rate. To achieve phase-matching in a tight focusing geometry, the scaling considerations that are described in the Ref. 10,11 are implemented. Basically, they relate important quantities, such as the HHG medium length and gas density, for different focusing geometries with the assumption that the same peak intensity, pulse duration, and central wavelength are used. Following these guidelines and using the recently demonstrated efficient HHG of post-compressed fiber lasers as a basis[21], a 65 μm nozzle size and xenon gas is chosen. Experimentally, the position of the gas nozzle relative to the focus and the backing pressure are optimized for maximum signal. This results in the jet being positioned as close as possible to the beam and slightly behind the focus, which guarantees that the short trajectories are phase-matched and that well-defined spatial profiles with low divergence are obtained[42]. For a better understanding of the phase-matching conditions, the signal of the harmonics is studied with respect to the backing pressure, e.g., for the two strongest harmonics H21 and H23 (Figure 3). As shown in Figure 3, the maximum signal is obtained at 1–1.2 bar, which is also in good agreement with the predictions of the scaling laws[10,11]. At these experimental conditions,

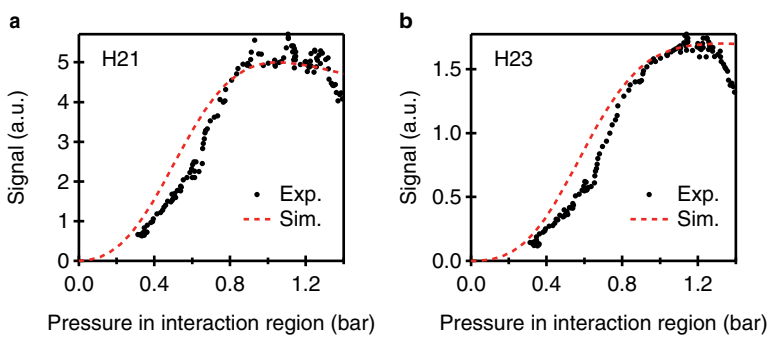

Figure 3 The signal of the 21st (**a**) and 23rd (**b**) harmonic is recorded for varying pressures (black dots). The signal build-up is compared with a phase-matching model (dashed red curves), which is described in the text.

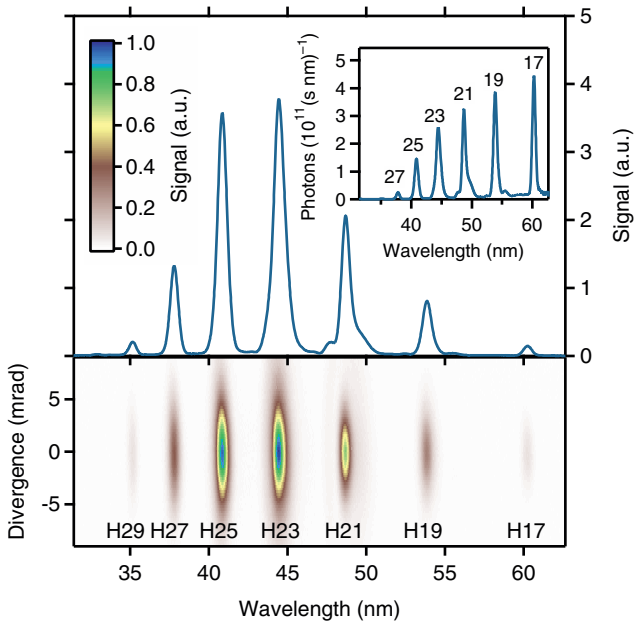

Figure 4 The spatially (x-axis) and spectrally (y-axis) resolved high harmonics generated at 234 kHz (lower panel). The experimental conditions are described in the text. The upper panel shows the spatial integration of the lower panel (inset: calibrated spectrum).

well-defined harmonics with a Gaussian beam profile are generated (Figure 4) as expected for phase-matched generation. The phase-matching conditions can be further investigated using a one-dimensional model that was introduced by Constant *et al.* and Kazamias *et al.*[43,44] This model calculates the signal of the qth harmonic on-axis and includes the pressure- and time-dependent wave-vector mismatch, $\Delta k(t,p) = q \times k_0 - k_q$, absorption effects and an empirical model of the single atom response[44]. The calculation of the wave-vector mismatch is performed at the focus position where the contribution of the dipole term, $(\Delta k_{\mathrm{dipole}} = -\alpha \times \partial I(z)/\partial z)$, vanishes.

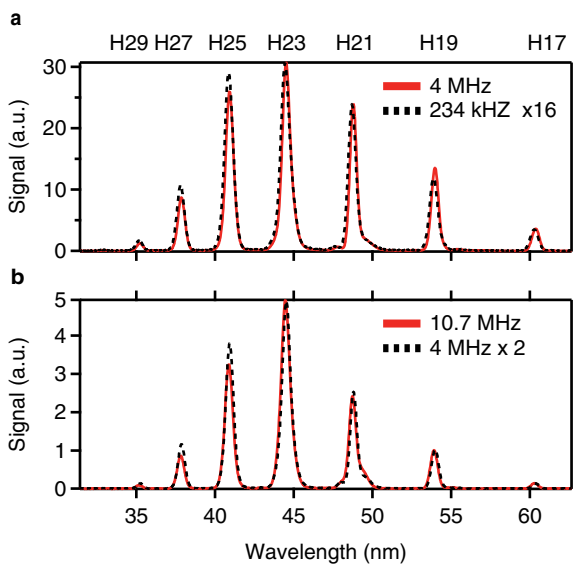

Figure 5 The signal of the high harmonics is compared for repetition rates of 234 kHz and 4 MHz (**a**) and 4 MHz and 10.7 MHz (**b**).

Table 1. HHG characteristics at a 10.7 MHz repetition rate

Harmonic order	H17	H19	H21	H23	H25
Wavelength (nm)	60	54	49	45	41
Average power (μW)	27.6	34.8	39.4	51.1	25.5
Photons s^{-1} (10^{12})	8.3	9.4	9.7	11.4	5.3
Conversion efficiency (10^{-7})	3.6	4.6	5.2	6.7	3.4

Further details on the calculation of the remaining terms are described elsewhere[9–11]. For the calculation a focal spot size radius of 11 μm ($1/e^2$-intensity), an intensity of 7.4×10^{13} W cm^{-2} and a Gaussian temporal envelope with a full width at half maximum duration of 30 fs are used. Additionally, we consider the residual absorption of the harmonics signal on its way to the detector as described in the supplementary information of the Ref. 21. The required ionization rates are calculated with the established model of Ammosov–Delone–Krainov (ADK)[45]. This calculation reveals that the intensity used leads to a fraction of ionized medium that is larger than the so-called critical ionization[9]. Therefore, the phase-matching condition is transiently fulfilled at the leading edge of the ultrashort laser pulse, where the coherence length, $(L_{\mathrm{coh}} = \pi/\Delta k)$, is longer than the medium length. The calculated harmonics signal (red dashed curves in Figure 3) shows good agreement with the measured signal with respect to the pressure in the interaction region. The pressure in the interaction region for the experimental data is obtained by scaling the recorded backing pressure using a gas-expansion model[11,46]. When phase-matching is achieved, the build-up of the harmonics is only limited by the linear absorption of the generation medium itself. Constant *et al.* have defined a criterion, i.e., $L_{\mathrm{med}} > 3L_{\mathrm{abs}}$ and $L_{\mathrm{coh}} > 5L_{\mathrm{abs}}$, under which the obtained harmonics signal is more than 50% of this asymptotic value[43]. The absorption lengths of the harmonics are $L_{\mathrm{abs}} = 15$ μm (H17), $L_{\mathrm{abs}} = 20$ μm (H19), $L_{\mathrm{abs}} = 26$ μm (H21), and $L_{\mathrm{abs}} = 30$ μm (H23) at the optimal experimental conditions[47], i.e., the maximum obtained signal. This means that the 17th and 19th harmonics are already absorption limited in their build-up. The upper panel of Figure 4 shows the obtained raw spectrum (spatially integrated) that was acquired by the CCD under the optimized conditions. When performing the calibration, the spectral shape changes (see inset of Figure 4) due to the aluminum filter transmission (see Supplementary Information). The calculation of the average power of the respective harmonics reveals that even at the low repetition rate of 234 kHz more than 1.5 μW (>3×10^{11} photons s^{-1}, inset of Figure 4) are generated in the strongest generated harmonic (H23, 27.7 eV).

After the HHG optimization, the scaling behavior with respect to the repetition rate was investigated (Figure 5). For this measurement, the two 200 nm thick aluminum filters (10 mm round aperture) are replaced by a 400 nm thick aluminum filter, which is mounted on a slit and can withstand a very high average power. First, the reference signal is recorded at 234 kHz and then compared with the signal obtained at 4 MHz, which is measured to be 16 times stronger (Figure 5a). Before further increasing the repetition rate, an additional 200 nm thick aluminum filter is inserted in the spectrometer chamber, which explains the change in the HHG spectrum in Figure 5b because aluminum absorbs stronger for the low harmonics (see Supplementary Figure S1). A new reference signal at 4 MHz is measured and compared with the signal obtained at the highest repetition rate of 10.7 MHz, showing another increase by a factor of 2 (Figure 5b). Using the overall obtained scaling factor of 32 and the calibrated measurement at 234 kHz (inset of Figure 4), the average power and conversion efficiency at 10.7 MHz can be determined. Table 1 lists these values for the 17th to the 25th harmonic. Remarkably, more than 50 μW of average

doi:10.1038/lsa.2015.93

power ($>10^{13}$ photons s^{-1}) is obtained in the strongest harmonic (H23, 27.7 eV), and all of these harmonics possess more than 20 μW ($>5 \times 10^{12}$ photons s^{-1}). The achieved conversion efficiency of up to 6.7×10^{-7} (H23) is close to the typical values (10^{-6}) achievable with other laser systems[44] and should be improvable by at least a factor of 2 by further optimizing the experimental conditions. The achieved photon flux is four orders of magnitude larger than that reported in studies on multi-MHz repetition rate HHG directly driven with a laser, i.e., without the additional enhancement cavity[28,29]. Moreover, the flux obtained in H23 is higher than what the state-of-the art enhancement cavities can deliver[8,24,31] and also exceeds the currently used kHz systems[30].

CONCLUSION

In summary, a promising novel source of high repetition rate coherent XUV radiation has been presented. Nonlinear compression in a Kagome PCF is utilized for achieving 7 μJ, 31 fs pulses at up to 10.7 MHz repetition rate. Furthermore, these pulses are used for efficient HHG in a 65 μm xenon gas jet. This results in a conversion efficiency of 6.7×10^{-7}, enabling more than 50 μW in a single harmonic ($>10^{13}$ photons s^{-1}), which is an improvement of four orders of magnitude compared with the reported multi-MHz systems of a single-pass HHG[28,29]. The photon flux is not only higher than what is supplied by current Ti:Sapphire technology[30] but also higher than intra-cavity HHG in the same wavelength range[8,24,31]. Additionally, the demonstrated repetition rate has previously been only accessible with enhancement cavities[23]. The achievement of efficient HHG with low-energy and high repetition rate laser systems has profound implications for a diverse field of HHG applications, e.g., in (multi)-dimensional surface science[48], coincidence detection[7], or coherent diffractive imaging[6,49]. Moreover, this experimental demonstration paves the way for making HHG sources more compact, cost-effective, reliable, and accessible to non-laser experts (e.g., by replacing our front-end (CC-FCPA) with a compact turn-key fiber laser system[33,34] or a thin-disk oscillator[35,36]). Future work will aim to combine state-of-the-art kilowatt class femtosecond lasers[15] with the presented compression scheme to achieve milliwatt-level harmonics. The realization of phase-matched HHG with an even tighter focus and the use of a carrier envelope phase and repetition rate stabilized driver will provide a source with a high photon flux (~100 μW per harmonic) with repetition rates of 40 MHz or more that could then be used for frequency metrology in the XUV.

ACKNOWLEDGEMENTS

This work was partly supported by the German Federal Ministry of Education and Research (BMBF) and the European Research Council under the European Union's Seventh Framework Programme (FP7/2007-2013)/ERC Grant Agreement No. 240460. Arno Klenke and Jan Rothhardt acknowledge financial support by the Helmholtz-Institute Jena.

1 Popmintchev T, Chen M-C, Arpin P, Murnane MM, Kapteyn HC. The attosecond nonlinear optics of bright coherent X-ray generation. *Nat Phot* 2010; **4**: 822–832.
2 Sansone G, Poletto L, Nisoli M. High-energy attosecond light sources. *Nat Phot* 2011; **5**: 655–663.
3 Südmeyer T, Marchese SV, Hashimoto S, Baer CRE, Gingras G *et al*. Femtosecond laser oscillators for high-field science. *Nat Phot* 2008; **2**: 599–604.
4 Mathias S, Bauer M, Aeschlimann M, Miaja-Avila L, Kapteyn HC *et al*. Time-resolved photoelectron spectroscopy at surfaces using femtosecond XUV pulses. In: Bovensiepen U, Petek H, Wolf M, editors. *Dynamics at Solid State Surface and Interfaces Vol.1: Current Developments*. Wiley-VCH Verlag GmbH & Co. KGaA; 2010. pp499–535.
5 Miao J, Sandberg R, Song C. Coherent X-ray diffraction imaging. *IEEE J Sel Top Quant Electron* 2012; **18**: 399–410.
6 Zürch M, Rothhardt J, Hädrich S, Demmler S, Krebs M *et al*. Real-time and Sub-wavelength Ultrafast Coherent Diffraction Imaging in the Extreme Ultraviolet. *Sci Rep* 2014; **4**: 7356.
7 Zhou X, Ranitovic P, Hogle CW, Eland JHD, Kapteyn HC *et al*. Probing and controlling non-Born-Oppenheimer dynamics in highly excited molecular ions. *Nat Phys* 2012; **8**: 232–237.
8 Cingöz A, Yost DC, Allison TK, Ruehl A, Fermann ME *et al*. Direct frequency comb spectroscopy in the extreme ultraviolet. *Nature* 2012; **482**: 68–71.
9 Paul A, Gibson EA, Zhang X, Lytle A, Popmintchev T *et al*. Phase-matching techniques for coherent soft X-ray generation. *Quantum Electron IEEE J* 2006; **42**: 14–26.
10 Heyl CM, Güdde J, L'Huillier A, Höfer U. High-order harmonic generation with μJ laser pulses at high repetition rates. *J Phys B At Mol Opt Phys* 2012; **45**: 074020.
11 Rothhardt J, Krebs M, Hädrich S, Demmler S, Limpert J *et al*. Absorption-limited and phase-matched high harmonic generation in the tight focusing regime. *New J Phys* 2014; **16**: 033022.
12 Schulz M, Riedel R, Willner A, Düsterer S, Prandolini MJ *et al*. Pulsed operation of a high average power Yb:YAG thin-disk multipass amplifier. *Opt Express* 2012; **20**: 5038–5043.
13 Saraceno CJ, Emaury F, Heckl OH, Baer CRE, Hoffmann M *et al*. 275 W average output power from a femtosecond thin disk oscillator operated in a vacuum environment. *Opt Express* 2012; **20**: 23535–23541.
14 Russbueldt P, Mans T, Weitenberg J, Hoffmann HD, Poprawe R. Compact diode-pumped 1.1 kW Yb:YAG Innoslab femtosecond amplifier. *Opt Lett* 2010; **35**: 4169–4171.
15 Eidam T, Hanf S, Seise E, Andersen TV, Gabler T *et al*. Femtosecond fiber CPA system emitting 830 W average output power. *Opt Lett* 2010; **35**: 94–96.
16 Boullet J, Zaouter Y, Limpert J, Petit S, Mairesse Y *et al*. High-order harmonic generation at a megahertz-level repetition rate directly driven by an ytterbium-doped-fiber chirped-pulse amplification system. *Opt Lett* 2009; **34**: 1489–1491.
17 Hädrich S, Krebs M, Rothhardt J, Carstens H, Demmler S *et al*. Generation of μW level plateau harmonics at high repetition rate. *Opt Express* 2011; **19**: 19374–19383.
18 Cabasse A, Machinet G, Dubrouil A, Cormier E, Constant E. Optimization and phase matching of harmonic generation at high repetition rate. *Opt Lett* 2012; **37**: 4618–4620.
19 Nisoli M, De Silvestri S, Svelto O. Generation of high energy 10 fs pulses by a new pulse compression technique. *Appl Phys Lett* 1996; **68**: 2793–2795.
20 Hädrich S, Klenke A, Hoffmann A, Eidam T, Gottschall T *et al*. Nonlinear compression to sub-30-fs, 0.5 mJ pulses at 135 W of average power. *Opt Lett* 2013; **38**: 3866–3869.
21 Hädrich S, Klenke A, Rothhardt J, Krebs M, Hoffmann A *et al*. High photon flux table-top coherent extreme ultraviolet source. *Nat Phot* 2014; **8**: 779–783.
22 Rothhardt J, Hädrich S, Klenke A, Demmler S, Hoffmann A *et al*. 53 W average power few-cycle fiber laser system generating soft x rays up to the water window. *Opt Lett* 2014; **39**: 5224–5227.
23 Ozawa A, Rauschenberger J, Gohle C, Herrmann M. High harmonic frequency combs for high resolution spectroscopy. *Phys Rev Lett* 2008; **100**: 253901.
24 Pupeza I, Holzberger S, Eidam T, Carstens H, Esser D *et al*. Compact high-repetition-rate source of coherent 100 eV radiation. *Nat Phot* 2013; **7**: 608–612.
25 Allison TK, Cingöz A, Yost DC, Ye J. Extreme nonlinear optics in a femtosecond enhancement cavity. *Phys Rev Lett* 2011; **107**: 183903.
26 Kim S, Jin J, Kim Y-J, Park I-Y, Kim Y *et al*. High-harmonic generation by resonant plasmon field enhancement. *Nature* 2008; **453**: 757–760.
27 Sivis M, Duwe M, Abel B, Ropers C. Extreme-ultraviolet light generation in plasmonic nanostructures. *Nat Phys* 2013; **9**: 304–309.
28 Vernaleken A, Weitenberg J, Sartorius T, Russbueldt P, Schneider W *et al*. Single-pass high-harmonic generation at 20.8 MHz repetition rate. *Opt Lett* 2011; **36**: 3428–3430.
29 Blättermann A, Chiang C, Widdra W. Atomic line emission and high-order harmonic generation in argon driven by 4-MHz sub-μJ laser pulses. *Phys Rev A* 2014; **89**: 043404.
30 Rundquist A, Durfee CG, Chang Z, Herne C, Backus S *et al*. Phase-matched generation of coherent soft X-rays. *Science* 1998; **280**: 1412–1415.
31 Pupeza I, Högner M, Weitenberg J, Holzberger S, Esser D *et al*. Cavity-enhanced high-harmonic generation with spatially tailored driving fields. *Phys Rev Lett* 2014; **112**: 103902.
32 Klenke A, Breitkopf S, Kienel M, Gottschall T, Eidam T *et al*. 530 W, 1.3 mJ, four-channel coherently combined femtosecond fiber chirped-pulse amplification system. *Opt Lett* 2013; **38**: 2283–2285.
33 Active Fiber Systems. Available at http://www.afs-jena.de (accessed 30 September 2014).
34 Amplitude Systémes. Available at http://www.amplitude-systemes.com (accessed 30 September 2014).
35 Saraceno CJ, Emaury F, Schriber C, Hoffmann M, Golling M *et al*. Ultrafast thin-disk laser with 80 μJ pulse energy and 242 W of average power. *Opt Lett* 2014; **39**: 9–12.
36 Brons J, Pervak V, Fedulova E, Bauer D, Sutter D *et al*. Energy scaling of Kerr-lens mode-locked thin-disk oscillators. *Opt Lett* 2014; **39**: 6442–6445.
37 Travers JC, Chang W, Nold J, Joly NY, St J Russell P. Ultrafast nonlinear optics in gas-filled hollow-core photonic crystal fibers [Invited]. *J Opt Soc Am B* 2011; **28**: A11–A26.
38 Emaury F, Dutin CF, Saraceno CJ, Trant M, Heckl OH *et al*. Beam delivery and pulse compression to sub-50 fs of a modelocked thin-disk laser in a gas-filled Kagome-type HC-PCF fiber. *Opt Express* 2013; **21**: 4986–4994.
39 Mak KF, Travers JC, Joly NY, Abdolvand A, St J Russell P. Two techniques for temporal pulse compression in gas-filled hollow-core kagomé photonic crystal fiber. *Opt Lett* 2013; **38**: 3592–3595.

40 Emaury F, Saraceno CJ, Debord B, Ghosh D, Diebold A *et al*. Efficient spectral broadening in the 100-W average power regime using gas-filled kagome HC-PCF and pulse compression. *Opt Lett* 2014; **39**: 6843–6846.
41 Möller M, Cheng Y, Khan SD, Zhao B, Zhao K *et al*. Dependence of high-order-harmonic-generation yield on driving-laser ellipticity. *Phys Rev A* 2012; **86**: 011401.
42 Salières P, L'Huillier A, Lewenstein M. Coherence control of high-order harmonics. *Phys Rev Lett* 1995; **74**: 3776–3779.
43 Constant E, Garzella D, Breger P, Mevel E, Dorrer C *et al*. Optimizing high harmonic generation in absorbing gases: model and experiment. *Phys Rev Lett* 1999; **82**: 1668–1671.
44 Kazamias S, Daboussi S, Guilbaud O, Cassou K, Ros D *et al*. Pressure-induced phase matching in high-order harmonic generation. *Phys Rev A* 2011; **83**: 063405.
45 Ammosov MV, Delone NB, Krainov VP. Tunnel ionisation of complex atoms and of atomic ions in an altering electromagnetic field. *Sov Phys JETP* 1986; **64**: 1191–1194.
46 Scoles G. *Atomic and Molecular Beam Methods*. Oxford University Press; 1988.
47 Henke BL, Gullikson EM, Davis JC. X-ray interactions: photoabsorption, scattering, transmission, and reflection at E=50-30000 eV, Z=1-92. *At Data Nucl Data Tables* 1993; **54**: 181–342.
48 Haarlammert T, Zacharias H. Application of high harmonic radiation in surface science. *Mater Sci* 2009; **13**: 13–27.
49 Sandberg RL, Paul A, Raymondson DA, Hädrich S, Gaudiosi DM *et al*. Lensless diffractive imaging using tabletop coherent high-harmonic soft-X-ray beams. *Phys Rev Lett* 2007; **99**: 098103.

Supplementary Information for this article can be found on the *Light: Science & Applications'* website (http://www.nature.com/lsa/).